

# Explosives Detection by Array of Si $\mu$ -Cantilevers Coated With Titanosilicate-Type Nanoporous Materials

Maria Pilar Pina Iritia, Fernando Almazán, Adela Eguizábal, Ismael Pellejero, Miguel Urbiztondo, Javier Sesé, Jesús Santamaría, Daniel García-Romeo, Belén Calvo, and Nicolás Medrano

*Invited Paper*

**Abstract**—An array comprising four Si  $\mu$ -cantilevers coated with nanoporous functionalized ETS-10 crystals sub-micrometric in size has been developed as a multisensing platform for explosives recognition in vapor phase. The detection capabilities of the proposed device have been tested for common taggants [such as 1-methyl-2-nitro-benzene (o-MNT)] and explosives (commercial detonation cord, a plastic tube filled with pentaerythritol tetranitrate (PETN); and C-4, a mixture of RDX, binders and plastifiers). The general strategy for the detection of explosives in vapor phase is based on the characteristic fingerprint each one produces as a result of the dissimilar chemical interactions between the ETS-10 coated  $\mu$ -cantilevers and the target molecules emanating from the explosives and swept by ambient air. A portable lock-in amplifier has been implemented to exploit the truly benefits of the array in terms of portability, reduced size, and energy consumption. Such low-power electronic interface is capable of creating the excitation signal as well as obtaining the response values of four resonating  $\mu$ -cantilevers simultaneously. The resulting sensing platform has successfully been applied for the o-MNT, PETN, and RDX detection at trace level.

**Index Terms**—ETS-10, explosives, gas sensing, nanoporous coatings, portable lock-in amplifier, o-MNT, PETN, RDX.

## I. INTRODUCTION

IDENTIFICATION and quantification of explosives have gained importance among emerging topics of research. In situ detection of explosives is of major importance for the public and private sector in several applications related to local law enforcement, homeland security and defense. In recent years, explosive-based terrorism has grown enormously since the use of improvised explosive devices (IEDs) is growing

Manuscript received April 27, 2015; revised June 16, 2015; accepted June 16, 2015. This work was supported by the Ministerio de Ciencia e Innovacion, Spain, under Grant CTQ2010-19276, Grant CTQ2013-49068, and Grant TEC2012-30802. The associate editor coordinating the review of this paper and approving it for publication was Prof. Kourosh Kalantar-Zadeh.

M. P. P. Iritia, F. Almazán, A. Eguizábal, I. Pellejero, M. Urbiztondo, J. Sesé, and J. Santamaría are with the Nanoscience Institute of Aragón, University of Zaragoza, Zaragoza 50018, Spain (e-mail: mapina@unizar.es; fer.almazan@me.com; adegui@unizar.es; ismapel@unizar.es; urbiz@unizar.es; jsese@unizar.es; jesus.santamaria@unizar.es).

D. García-Romeo, B. Calvo, and N. Medrano are with the Aragón Institute for Engineering Research, University of Zaragoza, Zaragoza 50018, Spain (e-mail: dgarcia.romeo@gmail.com; becalvo@unizar.es; nmedrano@unizar.es).

Color versions of one or more of the figures in this paper are available online at <http://ieeexplore.ieee.org>.

Digital Object Identifier 10.1109/JSEN.2015.2451732

In 2014, EU policy defined its own security strategy to respond to existing and emerging CBRN-E (Chemical, Biological, Radiological, Nuclear and Explosive) threats [1]. Accordingly, extensive efforts have been devoted to the development of innovative and effective detectors, capable of monitoring explosives both in time and location. Unfortunately, the reliable detection of explosives still represents a challenging task [2]. In theory, any chemical analysis scheme should be applicable for concealed explosives detection. Indeed, nearly all known instrumental methods have already been investigated for their applicability. However, none of the methods investigated to date solves the simultaneous problems of sensitivity, selectivity, reliability and speed required. This partly stems from the fact that explosives are composed of many chemicals, many being notoriously difficult to detect due to their physical and chemical properties. The main problem as far as vapor phase detection is concerned is their low vapor pressure in the pure form (from  $10^{-2}$  Pa to  $10^{-9}$  Pa at 298K). Then there is the problem of selectivity: the ability of the sensor to discriminate between explosive markers and a wide variety of volatile hydrocarbon products accompanying most modern travelers (cosmetics, parfums, synthetic fabrics...) must be guaranteed to avoid false alarms. The most effective and efficient method in current use is sniffing dogs [3], but they suffer from some limitations like behavioral variations and underperformance over time. Based on the same principle, the so called electronic nose—a device composed of hundreds of not highly selective and reversible chemical receptors located in an array format [4] that generates a response pattern mimicking the mammals olfaction system—outstands as one of the most promising alternative. The progress achieved in the field of chemical sensors during the last decades has been truly outstanding, leading to a continuous lowering of sensitivity limits. This has been driven in large part by the development of MEMS [5], [6]. Even though, commercial solutions for threats detection using MEMS technology are rarely available [7].

In view of the molecular recognition properties that nanoporous solids can achieve, our general strategy for reproducible and reliable vapor detection of explosives involves the combination of nanoporous sorbents as sensing materials and Si cantilevers provided with integrated heating elements as tiny microbalances. Particularly, zeolite type

nanoporous materials have been already deployed as sensing coatings on cantilevers due to their molecular recognition and highly tunable adsorption properties [8]–[11]. The potential of novel nanoporous framework materials, such as mixed octahedral-pentahedral-tetrahedral frameworks (OPT) containing different transition metals [12], has been scarcely explored for selective chemical detection. Owing to its wide-pore nature and thermal stability, ETS-10 is arguably the most important OPT microporous titanosilicate ( $\text{SiO}_4$ ,  $\text{TiO}_6$ ). Thus, the herein presented results on explosives detection are those obtained with ad-hoc synthesized ETS-10 type titanosilicates deposited over resonating Si  $\mu$ -cantilevers by evaporative microdropping technique. Special emphasis has been devoted to the study of post-synthesis treatments, i.e. surface functionalization and Ti enrichment, on the sorption properties and sensing performance.

## II. EXPERIMENTAL

### A. Microfabrication of Si $\mu$ -Cantilevers

The micromechanical structures herein used were fabricated from n-type SOI (silicon on insulator) wafers by using standard optical lithography and bulk micromachining technologies with five-levels of masks [13]. In general,  $\mu$ -cantilever sensors are configured to work as tiny microbalances with theoretical mass detection limits around 50 fg for standard fabricated devices. For dynamic mode operation, the effective mass change ( $\Delta m$ ) due to vapor sorption on the beam could be calculated from the resonance frequency changes ( $\Delta f$ ) by using the following equation (1):

$$\Delta m = S^{-1} \cdot \Delta f = \left( -r_n^{-1} \cdot L^3 w \sqrt{\frac{\rho^3}{E}} \Delta f \right) \quad (1)$$

where  $S$  is the theoretical mass sensitivity, and depends on: cantilever dimensions ( $L$  length and  $w$  width) and material properties ( $\rho$  density and  $E$  Young modulus); and frequency mode parameter ( $r_n = 0.1615$  for fundamental vibration mode). In this work,  $\mu$ -cantilevers 200  $\mu\text{m}$  wide, 15  $\mu\text{m}$  thick and from 500 to 535  $\mu\text{m}$  in length have been used. Thus, theoretical mass sensitivity ( $S$ ) values ranging from 16 to 20 Hz/ng are estimated from equation (1). With the final aim of miniaturization and integration, individual heating wires, actuation of the cantilever and mechanical resonance detection are integrated on each cantilever. The actuation is based on the induced Laplace electromagnetic force due to the coupling between the perpendicular magnetic field created by the magnet allocated on the chip basis and the electrical current passing through the coil patterned on the top surface of the  $\mu$ -cantilever. In order to detect the cantilever oscillation, semiconductor strain gauges are implanted at the surface of the microstructures which are arranged in half Wheatstone bridge configuration. A first gauge is localized where the stresses are maximum (the clamped-end of the beam); and the other reference gauge is on the rigid substrate.

### B. Low Power Electronic Interface for a Multi-Sensing Platform Comprising 4 $\mu$ -Cantilevers

A portable low-power electronic readout interface has been developed on ad hoc basis (Fig.1). Thus, the truly benefits of

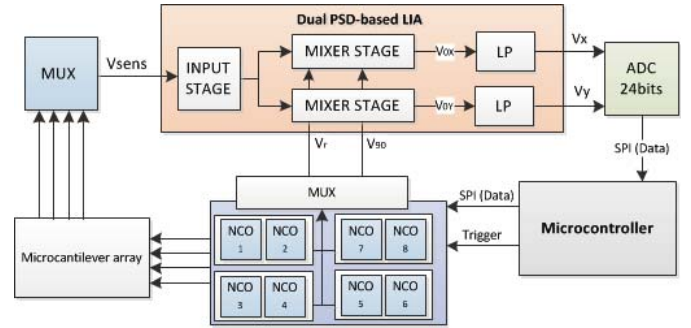


Fig. 1. Block diagram of the readout system.

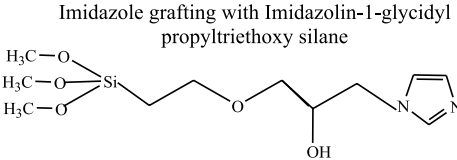
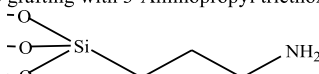
the multi-sensing platform in terms of portability, reduced size (110  $\times$  90  $\text{mm}^2$ ) and energy consumption (circa 69 mW while measuring) are greatly exploited. For this particular case, a suitable readout system must generate in parallel 4 different excitation signals at specific frequency values, which in fact, are continuously modified as a function of the gas phase composition and operating temperature. Furthermore, the 4  $\mu$ -cantilevers electrical outputs should be measured. To address this issue, the proposed electronic interface prototype, powered through a universal serial bus (USB) connected to a host computer, comprises the following three main blocks: i) a power supply that generates the DC levels required by both the sensors and the electronic interface; ii) a readout system based on a compact lock-in amplifier (LIA); and, iii) a microcontroller that manages the system operation: DC excitation for the piezoresistors, AC current bias for the actuation wire, system temperature control, frequency selection for the lock-in signals, LIA output reading and host computer communications.

The application of this technique to  $\mu$ -cantilever oscillation characterization has been already tested in [14] where the system was applied to a single cantilever. In order to extend the same solution to  $\mu$ -cantilever arrays, the new design must be capable of simultaneous sensor readout. In this particular case limited to 4  $\mu$ -cantilevers, a low cost low-power microcontroller Atmega 1281 is used. It controls the output frequency of the numerically controlled oscillators (NCO) that generate the four pairs of control signals required for the measurements. In addition, each pair of NCOs provides an excitation signal to its corresponding sensor. By properly multiplexing the output signal from the  $\mu$ -cantilever and one of the NCOs pairs, the compact LIA provides the corresponding measurements to the microcontroller. The core of the proposed portable readout block is a low-voltage low-power dual phase sensitive detection (PSD) based LIA. It carries out the data acquisition from the sensor output signals, thus recovering amplitude and phase values regardless of phase deviations produced by the sensors [15], [16]. This configuration, together with a new algorithm [15] capable of handling square signal as sensor excitation, constitutes a clear innovation for portable sensing systems.

### C. Titanosilicate Type Nanoporous Coating Preparation

Unlike zeolites, the basic properties of ETS-10 type nanoporous titanosilicates enlarge the variety of interactions

TABLE I  
SURFACE FUNCTIONALIZATION CONDITIONS FOR THE AS SYNTHESIZED ETS-10 TYPE TITANOSILICATES

| Organosilane  | Functionalization Procedure  |                     |   | $\frac{mmol_{organosilane}}{g_{ETS-10}}$ | Organosilane removal (K)** |
|---|--|---------------------|---|--|----------------------------|
|   | Zeolite (g) /organosilane (cm <sup>3</sup> ) /solvent (cm <sup>3</sup> ) | Reaction Conditions | Extraction Process                      |  |                            |
| Imidazole grafting with Imidazolin-1-glycidyl propyltriethoxy silane<br> | 1/9.5/47 (Cumene)  | T=425K, t=24h       | 2-Propanol (centrifugation and soxhlet) | 8.4                                      | 610                        |
| Amino grafting with 3-Aminopropyl triethoxysilane<br>                    | 1/10/150 (Toluene)   | T=383K, t=24h       | Ethanol (centrifugation)                | 0.2                                      | 628                        |

172 between the target molecules and the chemical receptors.  
 173 Owing to the framework-centered two-minus charge at the  
 174 Ti<sup>4+</sup> site, ETS-10 presents interesting opportunities to exploit  
 175 on the basis on its ion-exchange capability and low acidity.  
 176 Thus, the ETS-10 surface chemistry (Lewis base character) is  
 177 particularly adequate for sorption of electron acceptor  
 178 molecules, such as nitroderivates. In fact, acid-base interactions  
 179 (i.e. Meisenheimer complexes), and/or charge transfer  
 180 complexes formation (i.e.  $\pi$ - $\pi$  stacking) are those commonly  
 181 promoted for nitroderivates sensing [4], [17]. The porous structure  
 182 of ETS-10 is defined by 12-membered ring units along  
 183 the three dimensions. These are straight along [100] and [010]  
 184 (pore opening 0.49 nm  $\times$  0.76 nm) and crooked along the  
 185 direction of disorder. In this respect, ETS-10 exhibits excellent  
 186 diffusion characteristics for guest species.

187 For this work, ETS-10 (Si/Ti=5.5) submicrometric in  
 188 size, sample denoted as ETS-10\_1, has been hydrothermally  
 189 synthesized at 503 K during 24 h following the published  
 190 recipe by the authors [18]. The Ti enrichment of ETS-10,  
 191 sample denoted as ETS-10\_2, is based on reported protocols  
 192 for Al enrichment on zeolites [19]. Firstly a 0.05 M solution of  
 193 sodium metatitanate (99.9% Aldrich, 200 mesh) was prepared.  
 194 ETS-10\_1 powder was added to the prepared solution  
 195 (1:20 wt ratio), and kept under stirring during 10 min. Then,  
 196 sodium hydroxide pellets (Aldrich) were carefully added to  
 197 the solution until pH = 13, and kept under mechanical stirring  
 198 for 2 h at room temperature. Afterwards, the resulting solution  
 199 was put in a Teflon autoclave for recrystallization at 443K  
 200 during 12 hours.

201 The surface functionalization process is carried out over  
 202 as synthesized ETS-10 crystals by covalent linkage using  
 203 organosilanes as coupling agents. In particular, imidazolin-  
 204 1-glycidylpropyltriethoxysilane and 3-aminopropyltriethoxysilane  
 205 groups are grafted on the external nanoporous surface for the  
 206 preparation of IGPTS/ETS-10\_1 and NH<sub>2</sub>/ETS-10\_1 samples,  
 207 respectively. For such purposes, ETS-10\_1 powder, previously  
 208 dried under vacuum, is introduced in a three-neck round bottom  
 209 flask filled with Ar to avoid hydration. Then, anhydrous solvent  
 210 is injected and the resulting dispersion is sonicated for 15 minutes  
 211

TABLE II  
SYNTHESIZED NANOPOROUS TITANOSILICATES FOR  
NITRODERIVATES DETECTION

| Nomenclature              | Si/Ti atomic ratio* | H <sub>2</sub> O uptake (wt. %)** | S <sub>BET</sub> (m <sup>2</sup> /g) | Total Pore Volume Micropore Volume (cm <sup>3</sup> /g)/(cm <sup>3</sup> /g) |
|---------------------------|---------------------|-----------------------------------|--------------------------------------|--|
| ETS-10_1                  | 5.4                 | 7.9                               | 316                                  | 0.131/0.102  |
| ETS-10_2                  | 4.2                 | n.a.                              | 291                                  | 0.118/0.095  |
| IGPTS/ETS-10_1            | 5.4                 | 56.9                              | 95                                   | 0.090/n.a.   |
| NH <sub>2</sub> /ETS-10_1 | 5.4                 | 8.2                               | 216                                  | 0.102/0.073  |

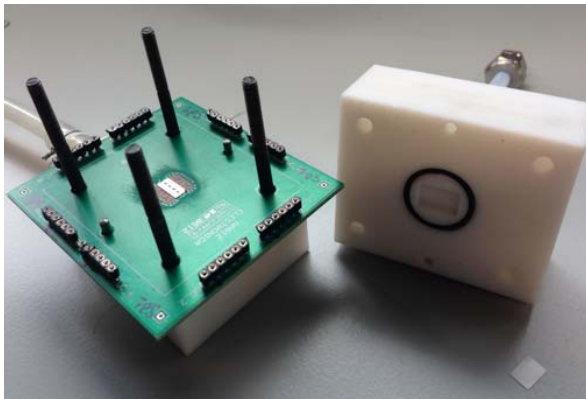
\*estimated by SEM-EDX; \*\*estimated by TGA in samples equilibrated at room conditions

212 under Ar atmosphere. Once the solvent reflux temperature  
 213 is achieved, the organosilane is added under mechanical  
 214 stirring and kept overnight. The specific conditions for  
 215 each functionalization procedure are shown in Table I.  
 216 Resulting materials were characterized by means of  
 217 energy-dispersive X-ray spectroscopy (SEM-EDX),  
 218 thermogravimetric analysis (TGA) for water uptake estimation  
 219 and Ar physisorption to evaluate composition and textural  
 220 properties: specific surface area for adsorption (S<sub>BET</sub>), and  
 221 total pore and micropore volume values, respectively. Table II  
 222 summarizes the main characteristics of the as prepared  
 223 solids.

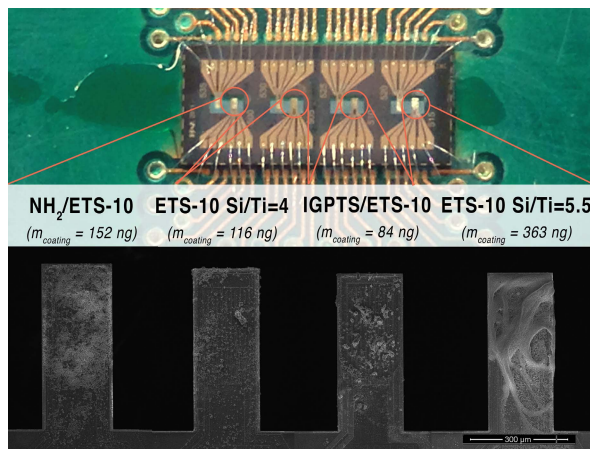
224 The Si  $\mu$ -cantilevers have been coated with ETS-10  
 225 crystals by evaporative microdropping technique [10], [11].  
 226 In particular, an ethanolic dispersion of each material (4% wt.)  
 227 is spread on the  $\mu$ -cantilever top surface using piezo-  
 228 driven inkjet printing technology (MD-E-201H, Microdrop  
 229 Technologies). For a proper control of the sensing material  
 230 location over the Si transducer, the instantaneous solvent  
 231 evaporation is induced during the dispensing process by means  
 232 of the meander-type heating resistor. This integrated heater is  
 233 also used at the end of the programmed detection sequences for  
 234 a proper degassing of the nanoporous materials to ensure the  
 235 full recovery of their sorption capabilities. Thus, regeneration  
 236 cycles (power consumption circa 300 mW), leading to average  
 237 temperature values on the beam circle 435 K, and 15 min

TABLE III  
MAIN CHARACTERISTICS OF THE ETS-10 MODIFIED  $\mu$ -CANTILEVERS

| Cantilever | Coating                   | $f_0$ (Hz) | $S$ (Hz/ng) | Coating loading (ng) |
|------------|---------------------------|------------|-------------|----------------------|
| 1          | ETS-10_1                  | 76290      | 18.2        | 363                  |
| 2          | ETS-10_2                  | 70870      | 17.2        | 116                  |
| 3          | IGPTS/ETS-10_1            | 77660      | 18.9        | 84                   |
| 4          | NH <sub>2</sub> /ETS-10_1 | 80520      | 20          | 152                  |



a)



b)

Fig. 2. a) Sensor chamber where the  $\mu$ -cantilever array is located. b) Top view of the Si  $\mu$ -cantilever array. SEM images of the ETS-10 coatings.

in duration have been systematically applied for a reliable and reproducible operation. Fig. 2.b shows the  $\mu$ -cantilever array where SEM insets for each modified beam have been also included. The main characteristics of the 4 coated Si  $\mu$ -cantilevers mostly used in this work are compiled in Table III. As it can be observed, the coating loading varies from 84 ng up to 363 ng. Consequently, the sensor's response has been normalized per mass of sensing material for a proper comparison.

#### D. Gas Sensing Measurements

The Si array comprising 4  $\mu$ -cantilevers pairs is firstly assembled on a PCB. Afterwards, it is placed in a custom sensor chamber with circa 1 cm<sup>3</sup> of free volume (see Fig. 2.a). The main gas inlet is distributed to four individual

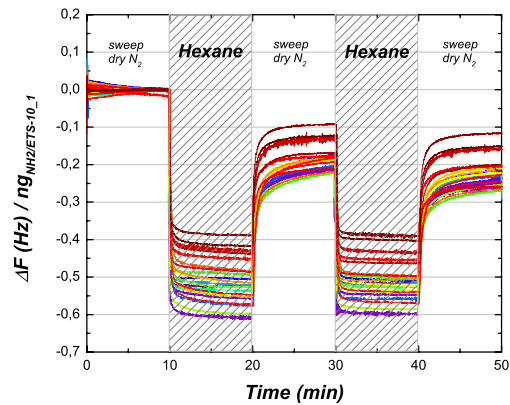


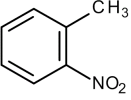
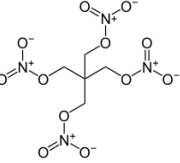
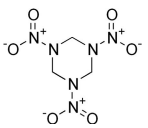
Fig. 3. Reproducibility of the response from four identical  $\mu$ -cantilevers coated with NH<sub>2</sub>/ETS-10\_1 subjected to C<sub>6</sub>H<sub>14</sub> detection (1000 ppmV) during consecutive sessions.

microchannels that deliver the gas stream to each  $\mu$ -cantilever pair. Thus, a cross-flow through the cantilever is ensured to maximize the interaction of the sample with the sensing elements. This gas-solid contact-mode configuration aims to reduce mass transfer limitations in the sorption process of target molecules present at trace level.

The platform was preliminary tested on the hexane detection to assess about the reproducibility of the measurements. For such purposes, samples from certified gas cylinder containing 1000 ppmV of n-C<sub>6</sub>H<sub>14</sub> in N<sub>2</sub> were evaluated. Fig. 3 summarizes the registered response values for four  $\mu$ -cantilevers all of them coated with NH<sub>2</sub>/ETS-10\_1. Each sensor was subjected to the same sensing cycle (10 min C<sub>6</sub>H<sub>14</sub>-10 min N<sub>2</sub>-10 min C<sub>6</sub>H<sub>14</sub>-10 min N<sub>2</sub>-final regeneration) during consecutive sessions (up to 9). The observed deviations for the steady-state response values towards 1000 ppmV of n-C<sub>6</sub>H<sub>14</sub> are mainly attributed to the distribution of the sensing material over the meander-type heating resistor. The ETS-10 location on the cantilever beam is clearly affecting the regeneration process, the sorption behavior, and consequently the sensor performance. It can be seen that the baseline is not fully regained during the 10 min measurement in dry N<sub>2</sub> (99.999 % purity). Accounting from the obtained results, the adsorption/desorption frequency shift ratio ( $\Delta f_{\text{ads}}/\Delta f_{\text{des}}$ ) has been identified as one of the most distinguished features of the chemical recognition process. The statistical analysis reveals  $\Delta f_{\text{ads}}/\Delta f_{\text{des}}$  values of  $1.54 \pm 0.12$  and  $1.13 \pm 0.03$  for the 1<sup>st</sup> and 2<sup>nd</sup> hexane step, respectively. Based on this parameter, the multisensing platform would accomplish with the criterion of reproducibility.

Table IV summarizes the main characteristics of the explosive related molecules studied in this work [20]. Firstly, the multisensing platform with cantilevers 1, 2, 3 and 4 (see Table III), was evaluated for 1-methyl-2-nitro-benzene (o-MNT) detection to verify the promoted sorption properties of the as prepared solids. This compound is recognized by the International Civil Aviation Organization as taggant for plastic bonded explosives. In this particular case, gas streams containing the desired species are prepared by bubbling N<sub>2</sub> (purity 99.999%) at set flowrates through saturator trains

TABLE IV  
PROPERTIES OF THE EXPLOSIVE RELATED COMPOUNDS  
TESTED IN THIS WORK

| Related/Explosives   | Molecular Structure   | Properties*  |
|--|---|--|
| 1-methyl-2-nitro-benzene (o-MNT)<br>$C_7H_7NO_2$                               |  | MW= 137.14 g/mol<br>Pv= $7.5 \times 10^{-4}$ Pa at 293 K<br>$T_{\text{decomposition}} = 543$ K                   |
| [3-nitrooxy-2,2-bis(nitrooxymethyl)propyl] nitrate (PETN)<br>$C_5H_8N_4O_{12}$ |  | MW=316.14 g/mol<br>Pv= $1.2 \times 10^{-8}$ Pa at 293 K<br>$T_{\text{decomposition}} = 414$ K<br>RE=1.66 TNTe/kg |
| 1,3,5-trinitroperhydro-1,3,5-triazine (RDX)<br>$C_3H_6N_6O_6$                  |  | MW=222.12 g/mol<br>Pv= $4.1 \times 10^{-9}$ Pa at 293 K<br>$T_{\text{decomposition}} = 443$ K<br>RE=1.6 TNTe/kg  |

\* RE factor refers to the amount of TNT (kg) equivalent to 1kg of the substance

kept at controlled temperature and further  $N_2$  dilution. Thus, concentration levels around 25 ppmV for o-MNT and 10000 ppmV for water ( $\sim 30\%$  RH at room temperature) in 80 mL(STP)/min of  $N_2$  are obtained.

Secondly, the multisensing platform was evaluated for two explosives widely used in both military and civil applications: detonation cord and C-4. Detonation cords are thin, flexible plastic tubes filled with PETN (pentaerythritol tetranitrate), with a relative effectiveness factor referred to TNT, denoted as RE, of 1.66. The C-4 is a common plastic explosive composed of 91% RDX (also known as cyclonite or hexogen), 5.3% plastifier (commonly diethylhexyl or dioctyl sebacate), 2.1% binder (polyisobutylene) and 1.6% SAE 10 non-detergent motor oil. Unlike o-MNT (liquid at room conditions), solid explosives detection fashion was performed in the lab simulating real field conditions. Thus, a small amount of explosive ( $\sim 500$  mg) was placed in a hermetic glass container of 2.5 L. In order to avoid high humidity conditions, the bottom of the recipient was filled with a desiccant material (silica gel). The challenging detection of explosives is further exacerbated by their inherently low vapor pressure:  $1.2 \times 10^{-8}$  Pa in the case of PETN and  $4.1 \times 10^{-9}$  Pa for RDX at room conditions. For the sensing experiments herein performed, the solid samples were heated up to 343K to increase the generation of vapors emanating from the solids.

Like currently available trace detection systems, the inlet sample contains the air from the vicinity of the solid. Sample collection is performed on the glass container with the aid of a micro air pump (Xavitech®AB), which pulls the sample into the sensor chamber (see Fig. 4). Due to the hydrophilic properties of the sensing materials (water uptake values ranging from 7.9% up to 56.9% wt), the ETS-10 nanoporous coatings were carefully regenerated with anhydrous air

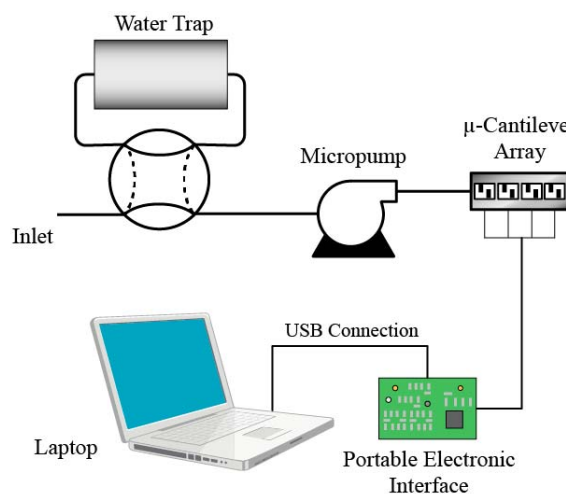


Fig. 4. Experimental layout for the prototype testing with real solid explosives.

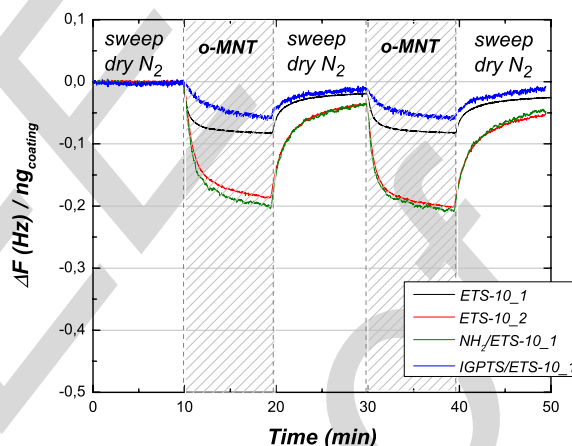


Fig. 5. Evolution of the resonance frequency shift of the multisensing platform in presence of o-MNT (25 ppmV).

previous to any sensing experiment with real explosives. For such purposes, the sweeping air was pumped through a radial fixed bed sorbent trap of commercial zeolite 3A beads (Si/Al=1.55).

### III. RESULTS AND DISCUSSION

#### A. o-MNT Detection in Synthetic Gas Mixtures

Fig. 5 shows the frequency shift variation of the multisensing platform upon the introduction of two consecutive o-MNT (25 ppmV) steps 10 min in duration with an intermediate  $N_2$  flushing. Similar experiments, not shown here, were carried out for water (10000 ppmV). The main parameters derived from such measurements are summarized in Table V.

As it was expected, the surface properties affect on sensor's response. Among the studied functionalization procedures, the amino grafting (NH<sub>2</sub>/ETS-10\_1) and the Ti enrichment (ETS-10\_2) lead to affinity enhancement towards o-MNT compared to pristine counterpart (ETS-10\_1). The sorption capability of amino grafted sample is 2.6 fold higher than the

TABLE V  
SENSING PERFORMANCE OF ETS-10 MODIFIED  $\mu$ -CANTILEVERS FOR  
SINGLE o-MNT AND WATER DETECTION

| Cantilever | Coating                   | o-MNT Detection* |                                 |                                  | H <sub>2</sub> O as interference |
|------------|---------------------------|------------------|---------------------------------|----------------------------------|----------------------------------|
|            |                           | $t_1$ (s)        | $\Delta f_{ads}/\Delta f_{des}$ | $\frac{ng_{o-MNT}}{ng_{ETS-10}}$ | $\frac{ng_{H_2O}}{ng_{ETS-10}}$  |
| 1          | ETS-10_1                  | 46               | 1.25                            | 0.5 %                            | 1.8 %                            |
| 2          | ETS-10_2                  | 69               | 1.07                            | 0.9 %                            | 3.5 %                            |
| 3          | IGPTS/ETS-10_1            | 184              | 1.35                            | 0.3 %                            | 17.3 %                           |
| 4          | NH <sub>2</sub> /ETS-10_1 | 78               | 1.45                            | 1.3 %                            | 5.6 %                            |

\*calculated from the first o-MNT step.

345 exhibited by bare titanosilicate (1.3% wt. versus 0.5%wt for  
346 NH<sub>2</sub>/ETS-10\_1 and ETS-10\_1 respectively). This behavior is  
347 explained on the basis of the electron deficient character of  
348 the nitroaromatic explosive, and the electron donor properties  
349 of grafted amine groups [4], [17]. A similar effect,  
350 but less notorious, is observed for the Ti enriched  
351 coating (ETS-10\_2). The basic properties promotion leads  
352 to charge transfer from Ti<sup>4+</sup> to the aromatic ring and  
353 electron-withdrawing nitro group. This coating presents  
354 o-MNT pseudoequilibrium value of 0.9% wt. versus 0.5%wt  
355 for pristine ETS-10\_1.

356 On the other hand, the imidazole grafted sample,  
357 IGTPS/ETS-10\_1, is the less sensitive towards o-MNT. This  
358 fact is attributed to its extremely high functionalization degree  
359 (up to 8.4 mmol of grafted organosilane per g of ETS-10).  
360 Based on Ar physisorption analysis, the volume of micropores  
361 in pristine ETS-10\_1 sample, circa 78% of total pore volume,  
362 becomes negligible after imidazole grafting. Our explanation  
363 relies on the micropore clogging by hydrated organosilane  
364 molecules grafted on the external surface of the crystals.  
365 This bulky network hinders the diffusion of target analytes  
366 through the ETS-10 microporous framework. Among the  
367 tested, NH<sub>2</sub>/ETS-10\_1 represents the optimal trade-off  
368 between external surface modification and exposed volume of  
369 micropores.

370 The response recovery after N<sub>2</sub> flushing, expressed as  
371  $\Delta f_{ads}/\Delta f_{des}$ , for the cantilever modified with NH<sub>2</sub>/ETS-10\_1  
372 is the less pronounced. This observation is related to the sorption  
373 heat involved [13] and underlines the importance of degassing  
374 conditions [11] for a reusable, reliable multisensing platform  
375 for explosives. The regeneration protocols herein used ensure  
376 the recovery of the sorption capacity for the ETS-10 deposits  
377 over the heating resistor.

378 In a step further and with the final aim to characterize the  
379 sorption kinetics from single o-MNT experimental results, the  
380 following equation (2) has been used:

$$381 \quad Y = Y_{eq} \left(1 - e^{-\frac{t}{t_1}}\right) \quad (2)$$

382 where:  $Y_{eq}$  (ng<sub>ads</sub>/ng<sub>coating</sub>) is the amount of sorbate molecules  
383 per ETS-10 sorbent under pseudo equilibrium conditions, for  
384 a given analyte concentration in the gas phase; and,  $t_1$  is  
385 the time required to reach an average amount of sorbate  
386 equals to  $0.63 \cdot Y_{eq}$ . As can be seen in Table V, the kinetic

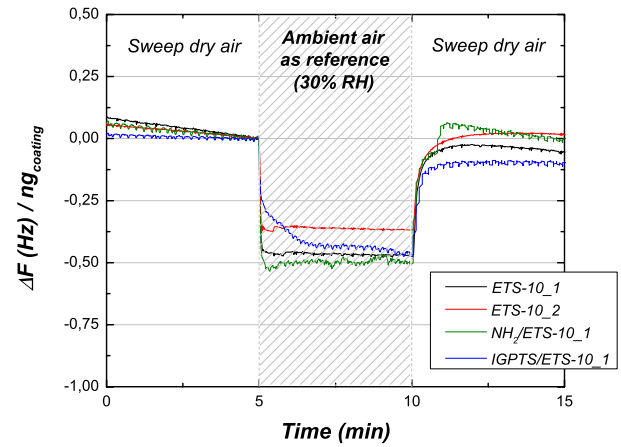


Fig. 6. Evolution of the resonance frequency shift of the multisensing platform in presence of ambient air (blank assay).

387 response of each one of them is clearly different. Thus, both  
388  $Y_{eq}$  and  $t_1$  parameters, together with the response recovery  
389 ( $\Delta f_{ads}/\Delta f_{des}$ ), outstand as the most relevant features  
390 of the molecular fingerprint provided by our platform. The  
391 cantilever 1 shows the faster response due to the higher specific  
392 surface area of the ETS-10\_1 coating (316 m<sup>2</sup>/g). Excluding  
393 cantilever 3 modified with IGTPS/ETS-10\_1, all the sensors  
394 show  $t_1$  values less than 80 s. Recent efforts are focused on a  
395 more compact system design to reduce dead volume with the  
396 final aim to improve response time.

397 From the set of o-MNT experiments, the calculated  
398 gas sensitivity values ranges from 0.19 Hz/ppmV in  
399 cantilever 3 to 1.58 Hz/ppmV for cantilever 4. Accounting  
400 from the experimental signal noise of the portable system,  
401 limit of detection (LOD) values below 2 ppmV are obtained  
402 for cantilever 4. In general, the sensing performance of the  
403 as prepared titanosilicates is worse than the already reported  
404 for Co exchanged BEA type zeolites [13], [14] under similar  
405 conditions ( $\sim 0.1$  ppmV).

406 The water sorption on the ETS-10 nanoporous coatings  
407 has also been analyzed due to the unavoidable presence of  
408 humidity as interference. It is found that all the post-synthesis  
409 treatments increase the water uptake (see Table V).  
410 However, this effect is quite remarkable for amino-grafted  
411 and imidazole-grafted samples in agreement with the intrinsic  
412 properties of the coupling organosilanes. Especially noticeable  
413 is the behavior of cantilever 3 coated with  
414 IGTPS/ETS-10\_1. The water pseudoequilibrium value at  
415 10000 ppmV is 17.3% wt. versus 1.8%wt for pristine  
416 ETS-10\_1. Such hydrophilicity, rather similar to Al-enriched  
417 zeolites, is explained by the hydrogen bonding network  
418 provided by the organosilane molecules (with ether, hydroxyl  
419 and imidazole functions) anchored on the crystal surface.  
420 This observation is also consistent with the TGA results  
421 shown in Table II.

### 422 B. Field Testing With Real Explosives

423 Unlike previously, the multisensing platform performance  
424 working like hand-held detection systems (see Fig. 4) is  
425 depicted in Fig. 6., Fig. 7, and Fig. 8.

TABLE VI  
SENSING PERFORMANCE OF ETS-10 MODIFIED  $\mu$ -CANTILEVERS FOR PETN AND C-4 DETECTION

| Cantilever | Coating                   | PETN                          |  |            | C-4                           |  |            |
|------------|---------------------------|-------------------------------|--|------------|-------------------------------|--|------------|
|            |                           | $\frac{n_{ads}}{ng_{ETS-10}}$ | $\frac{\Delta f_{ads}}{\Delta f_{background}}$ | $t_1$ (s)* | $\frac{n_{ads}}{ng_{ETS-10}}$ | $\frac{\Delta f_{ads}}{\Delta f_{background}}$ | $t_1$ (s)* |
| 1          | ETS-10_1                  | 1.8 %                         | 0.63   | 5          | 2.6 %                         | 0.90   | 3          |
| 2          | ETS-10_2                  | 1.5 %                         | 0.59   | 3          | 2.5 %                         | 1.19   | 7          |
| 3          | IGPTS/ETS-10_1            | 2.9 %                         | 1.14   | 60         | 1.9 %                         | 0.75   | 15         |
| 4          | NH <sub>2</sub> /ETS-10_1 | 4.4 %                         | 1.55   | 5          | 3.9 %                         | 1.40   | 7          |

\*Theoretical pseudo-equilibrium constant time (Equation 2)

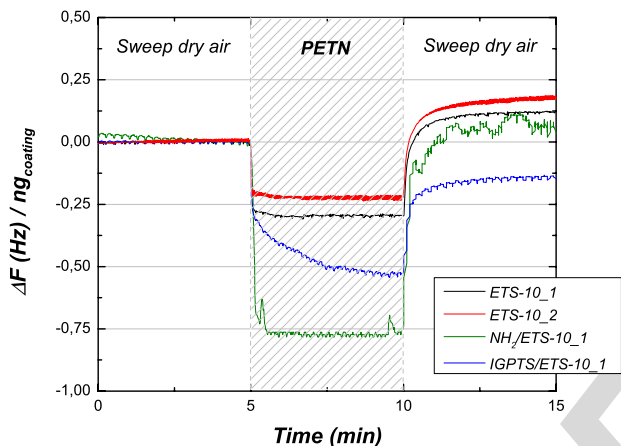


Fig. 7. Evolution of the resonance frequency shift of the multisensing platform in presence of vapors emanating from solid PETN at 343K.

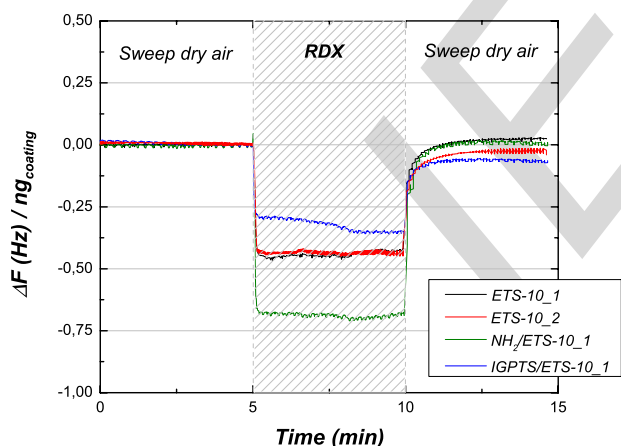


Fig. 8. Evolution of the resonance frequency shift of the multisensing platform in presence of vapors emanating from solid C-4 at 343K.

In particular, Fig. 6. shows the multisensing platform response to ambient air from the lab, used as reference. Despite the humidity content was rather similar to the previously studied in Table V, the observed tendencies are notably different. Working with complex environments involves a great number of unknown factors difficult to identify. Thanks to this blank assay, the reference baseline for each individual microsensor is established and conveniently used to discard the interferences from the background.

Similarly, Fig. 7. and Fig. 8. show the responses to the vapors emanating from PETN and C-4 solids

at 343 K, respectively. As previously, the cantilever 4 coated with NH<sub>2</sub>/ETS-10\_1 exhibits the most outstanding performance in both scenarios dealing with solid explosives. In principle, this behavior matches with the presence of 4 and 3 electron-withdrawing nitro groups in PETN and RDX molecules, respectively. However, the steady-state response towards each vapor mixture does not differ substantially. Once again, this observation underlines the importance of acquiring numerous molecular properties on a single measurement mode for a reliable classification. When comparing with the blank assay results (see Fig. 6.), the response of cantilever 3 towards PETN seems quite similar. On the contrary, the response to RDX is even smaller than the reference baseline. This behavior could be explained by the hygroscopic character of some explosives. Thus, the C-4 solid would behave as desiccant during the sample collection step. Above all, it should be taken into account that the tested explosives are essentially a complex mixture where plastifiers and binders are commonly present. These additives, with substantial vapor pressure, may act as interferences in the recognition of the energetic materials.

Table VI compiles the values for  $y_{eq}$  and  $t_1$  of the multisensing platform upon exposure to the vapours emanating from PETN and C-4 materials at 343K. One of the most outstanding features is the improved response time of the platform. The evaluated  $t_1$  values, with the exception of those registered for IGPTS/ETS-10\_1 coating, are always below 10s. This behavior is due to the micropump pulling (circa 500 mL(STP)/min) and the solid heating which increases the vapor pressure of the molecules eluted from the tested material. In spite of the huge differences in vapor pressure of o-MNT, PETN and RDX species (see Table IV), the pseudo-equilibrium sorption values for real solid explosives are higher than for taggants. In fact, what it may be recognizing is not the explosive related molecules, and mainly the concomitant additives. From the results herein obtained, it is difficult to establish a direct correlation among the concentration of the energetic substance and the  $y_{eq}$  and  $t_1$  parameters. For such purposes, a comprehensive characterization of the multisensing platform as a function of the solid temperature during sample collection would be required.

### C. Explosives Recognition by Their Fingerprint

The previous experiments show the specific responses of each  $\mu$ -cantilever upon the exposure to different species in the

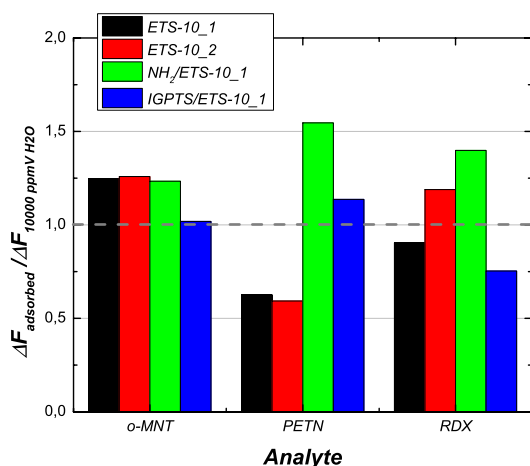


Fig. 9. Differential responses of the ETS-10 modified  $\mu$ -cantilevers upon exposure to vapors of o-MNT (25 ppmV), PETN (solid at 343K) and C-4 (solid at 343K).

gas phase. Although most of the results can be qualitatively explained on the basis of chemical interactions, some behaviors diverge from what it is expected due to the complexity of the explosive mixture. Since a detailed study of each single possible molecular interaction with certain species in the gas phase is unaffordable, our sensing approach deals with the analysis of the overall fingerprint.

For the purposes of this work, the  $\Delta f_{\text{ads}}/\Delta f_{\text{background}}$  ratio (see Table VI) is identified as the characteristic parameter of the sensor performance with complex mixtures. This value reflects the differential response due to presence of additional extra species not present in the background (i.e. ambient air in the proximity of the solid explosive). Fig. 9 shows the as calculated values for the PETN and C-4 detection sequences. The experiments with the o-MNT taggant, analyzed on a similar basis, have been also included for a proper comparison. It is found that cantilever 4 coated with NH<sub>2</sub>/ETS-10\_1 always reacts under the presence of nitro compounds, independently of the complexity of the ambient. For ETS-10\_1 and ETS-10\_2 coatings, unexpected responses towards nitro based explosive compounds are observed due to the contribution of chemical interactions with the concomitant additives. In the case of hydrophilic IGPTS/ETS-10\_1 coating, the response seems to be highly conditioned by the hygroscopic character of the solids.

Due to the fact that each sensing nanoporous material classifies the complex vapor phase according to sorbent-sorbate molecular interactions, it is not necessary to identify each one of the individual chemical species. In our case, specific fingerprints have been obtained for three explosive-related molecules with a multisensing platform comprising four different  $\mu$ -cantilevers. Undoubtedly, this approach can be naturally extended to dozens of  $\mu$ -cantilevers for redundancy and reliability.

#### IV. CONCLUSIONS

Nanoporous ETS-10 type titanosilicates with promoted sorption properties towards nitroderivates type explosives have been synthesized. By using microdropping technique,

an array comprising 4 Si  $\mu$ -cantilevers coated with such ETS-10 crystals has been prepared. The detection capabilities of the multisensing platform have been successfully validated for o-MNT taggant detection and two common explosives: detonation cord filled with PETN, and C-4 plastic explosive containing RDX. The experimental adsorption-desorption frequency shift ratio ( $\Delta f_{\text{ads}}/\Delta f_{\text{des}}$ ), and response time ( $t_1$ ) defined for the 63% of the maximum signal have been identified as the most relevant features of the molecular fingerprint provided by the platform. For field testing, the  $\Delta f_{\text{ads}}/\Delta f_{\text{background}}$  ratio outstands as the characteristic parameter to discard the interferences from the surrounding air. The multisensing platform comprising four different  $\mu$ -cantilevers leads to specific patterns for the three explosive-related molecules. Among the tested, the cantilever 4 coated with NH<sub>2</sub>/ETS-10\_1 material exhibits the most outstanding performance due to the electron deficient character of the nitroderivates, and the electron donor properties of grafted amine groups.

#### REFERENCES

- [1] *The EU Internal Security Strategy in Action: Five Steps Towards a More Secure Europe*, 2010, p. 673.
- [2] *Observatory NANO Security Report*. [Online]. Available: [http://www.nanopinion.eu/sites/default/files/ts\\_security\\_sub-sector\\_-\\_explosive\\_detection\\_may\\_09.pdf](http://www.nanopinion.eu/sites/default/files/ts_security_sub-sector_-_explosive_detection_may_09.pdf), accessed Apr. 2015.
- [3] [Online]. Available: <http://swgdog.fiu.edu/>, accessed Apr. 2015.
- [4] A. Lichtenstein *et al.*, "Supersensitive fingerprinting of explosives by chemically modified nanosensors arrays," *Nature Commun.*, vol. 5, p. 4195, Jun. 2014.
- [5] B. Rogers, S. Malekos, L. Deal, R. Whitten, and J. Adams, "Combined, solid-state molecular property and gamma spectrometers for CBRN&E detection," in *Proc. IEEE Int. Conf. Technol. Homeland Secur.*, Waltham, MA, USA, Nov. 2013, pp. 607–612.
- [6] A. Boisen, S. Dohn, S. S. Keller, S. Schmid, and M. Tenje, "Cantilever-like micromechanical sensors," *Rep. Prog. Phys.*, vol. 74, no. 3, p. 036101, 2011.
- [7] [Online]. Available: <http://www.nevadanano.com/>, accessed Apr. 2015.
- [8] M. A. Urbiztondo *et al.*, *Ordered Porous Solids*. Oxford, U.K.: Elsevier, 2009, pp. 381–401.
- [9] M. P. Pina *et al.*, "Zeolite films and membranes. Emerging applications," *Microporous Mesoporous Mater.*, vol. 144, nos. 1–3, pp. 19–27, Oct. 2011.
- [10] M. A. Urbiztondo *et al.*, "Zeolite-modified cantilevers for the sensing of nitrotoluene vapors," *Sens. Actuators B, Chem.*, vol. 137, no. 2, pp. 608–616, Apr. 2009.
- [11] M. A. Urbiztondo *et al.*, "Detection of organic vapours with Si cantilevers coated with inorganic (zeolites) or organic (polymer) layers," *Sens. Actuators B, Chem.*, vols. 171–172, pp. 822–831, Aug./Sep. 2012.
- [12] J. Rocha and M. W. Anderson, "Microporous titanosilicates and other novel mixed octahedral-tetrahedral framework oxides," *Eur. J. Inorganic Chem.*, vol. 2000, no. 5, pp. 801–818, 2000.
- [13] I. Pellejero, A. Peralta, M. A. Urbiztondo, J. Sese, M. P. Pina, and J. Santamaria, "Explosives detection by using 8-microcantilever chips with self-heating elements modified with exchanged BEA type zeolites," in *Proc. 17th TRANSDUCERS EUROSENSORS*, Barcelona, Spain, Jun. 2013, pp. 262–265.
- [14] D. García-Romeo *et al.*, "Portable low-power electronic interface for explosive detection using microcantilevers," *Sens. Actuators B, Chem.*, vol. 200, pp. 31–38, Sep. 2014.
- [15] J. Aguirre, N. Medrano, B. Calvo, and S. Celma, "Lock-in amplifier for portable sensing systems," *Electron. Lett.*, vol. 47, no. 21, pp. 1172–1173, 2011.
- [16] J. Aguirre, D. García-Romeo, N. Medrano, B. Calvo, and S. Celma, "Square-signal-based algorithm for analog lock-in amplifiers," *IEEE Trans. Ind. Electron.*, vol. 61, no. 10, pp. 5590–5598, Oct. 2014.
- [17] Y. Engel, R. Elnathan, A. Pevzner, G. Davidi, E. Flaxer, and F. Patolsky, "Supersensitive detection of explosives by silicon nanowire arrays," *Angew. Chem. Int. Ed.*, vol. 49, no. 38, pp. 6830–6835, 2010.

- 587 [18] A. Eguizábal *et al.*, “Novel hybrid membranes based on polybenzimidazole and ETS-10 titanasilicate type material for high temperature  
588 proton exchange membrane fuel cells: A comprehensive study on dense  
589 and porous systems,” *J. Power Sour.*, vol. 196, no. 21, pp. 8994–9007,  
590 2011.  
591
- 592 [19] K. Shanjiao, D. Tao, L. Qiang, D. Aijun, Z. Yanying, and P. Huifang,  
593 “Preparation and application of zeolite beta with super-low SiO<sub>2</sub>/Al<sub>2</sub>O<sub>3</sub>  
594 ratio,” *J. Porous Mater.*, vol. 15, no. 2, pp. 159–162, 2008.
- 595 [20] E. J. Staples, *Electron. Sensor Technol.*, Newbury Park, CA, USA,  
596 Tech. Rep., 2003.

597 **Maria Pilar Pina Iritia** received the Ph.D. degree in chemistry from the  
598 University of Zaragoza, Spain, in 1997. She became a Tenure Associate  
599 Professor with the Department of Chemical and Environmental Engineering,  
600 University of Zaragoza, in 2007. Her current research pivotes on microsystems  
601 development based on nanostructured materials for reaction, separation, and  
602 sensing applications.

603 **Fernando Almazán** received the M.Sc. degree in biomedical engineering  
604 from the University of Zaragoza, in 2012. He is currently pursuing the  
605 Ph.D. degree in chemical engineering with the Nanoscience Institute of  
606 Aragon. His research interests include microsystems and microfluidic devices  
607 fabrication and their application for gas sensing at trace level.

AQ:9 608 **Adela Eguizábal** received the Ph.D. degree in chemical engineering from  
609 the University of Zaragoza in 2013. She is currently a Researcher with the  
610 Nanotechnology Department, The Footwear Technology Center of La Rioja.  
611 Her research interests are focused on the incorporation of nanostructured  
612 materials and ionic liquids on polymer-based microsystems for microreaction,  
613 gas sensing, and PEMFC applications.

614 **Ismael Pellejero** received the Ph.D. degree in chemical engineering from the  
615 University of Zaragoza in 2012. He is currently a Research Associate with  
616 the Department of Chemical and Environmental Engineering and also with  
617 the Nanoscience Institute of Aragon. His research interests are nanostructured  
618 material and microsystems fabrication, mainly sensors, and microfluidic  
619 devices.

620 **Miguel Urbiztondo** received the Ph.D. degree in chemical engineering from  
621 the University of Zaragoza in 2008. He is currently an Associate Professor  
622 with the University Centre for Defence Studies and also with the Nanoscience  
623 Institute of Aragón. His research interests are in the area of nanoporous  
624 materials, in particular, in microfabricated zeolitic devices for chemical sensor  
625 applications.

**Javier Sesé** received the Ph.D. degree in physics from the University of  
626 Zaragoza in 1999, with a focus on applied superconductivity in quantum  
627 metrology. From 2000 to 2004, he was involved in the development of new  
628 microelectromechanical systems (MEMS) for electrical metrology with the  
629 MESA+ Institute for Nanotechnology, The Netherlands. He was awarded the  
630 Ramón y Cajal contract in the Nanoscience Institute of Aragón in 2004, where  
631 he is in charge of the Laboratory of Microlithography. His current research  
632 interests include the MEMS development for superconducting and gas sensors.  
633

**Jesús Santamaría** received the Ph.D. degree in chemical engineering from  
634 the University of Salford, U.K., in 1985. In 1990, he became a Professor  
635 of Chemical Engineering with the University of Zaragoza, where he is in  
636 charge of the Nanoporous Films and Particles Research Group. His research  
637 activities are in the field of nanostructured materials (nanoparticles, interfaces,  
638 and catalysts), and their applications in microreactors, gas sensors, and  
639 nanomedicine. He is currently one of the editors of the *Chemical Engineering*  
640 *Journal*, and the Vice Director of the Nanoscience Institute of Aragon.  
641

**Daniel García-Romeo** received the Degree in electronics engineering from  
642 the University of Zaragoza, where he is currently pursuing the Ph.D. degree  
643 with the Group of Electronic Design, Aragon Institute for Engineering  
644 Research (GDE-I3A), University of Zaragoza. His research interests include  
645 integrated sensor interfaces, signal processing, and intelligent instrumentation.  
646

**Belén Calvo** received the B.Sc. degree in physics and the Ph.D. degree in electronics  
647 engineering from the University of Zaragoza, Spain, in 1999 and 2004,  
648 respectively. She is a Senior Researcher with the Group of Electronic  
649 Design, Aragon Institute for Engineering Research (GDE-I3A), University  
650 of Zaragoza. Her research interests include low-voltage low-power analog  
651 and mixed-mode CMOS design strategies, implementation and test of recon-  
652 figurable smart sensor-to-microcontroller ASIC interfaces, wireless sensors  
653 networks, and wideband front-end IC transceivers.  
654

**Nicolás Medrano** received the B.Sc. and Ph.D. degrees in physics from the  
655 University of Zaragoza, Zaragoza, Spain, in 1989 and 1998, respectively. He is  
656 currently an Associate Professor of Electronics with the Faculty of Physics  
657 and a member of the Group of Electronic Design with the Aragon Institute of  
658 Engineering Research, University of Zaragoza. His current research interests  
659 include adaptive signal processing, integrated sensor interfaces, wireless  
660 sensor networks, and intelligent instrumentation.  
661

## AUTHOR QUERIES

AQ:1 = Please provide the expansion for “RDX.”

AQ:2 = Please confirm the postal code for “University of Zaragoza.”

AQ:3 = Please confirm the title. Also provide the organization and location for ref. [1].

AQ:4 = Please confirm the title and URL address for ref. [2].

AQ:5 = Please provide the title for refs. [3] and [7].

AQ:6 = Please confirm the author names for ref. [8].

AQ:7 = Please confirm the volume no. for ref. [12].

AQ:8 = Please confirm the author name, organization, and location. Also provide the title for ref. [20].

AQ:9 = Current affiliation in biography of “Adela Eguizábal” does not match First Footnote. Please check.

IEEE  
Proof